

Gephyrin-Independent GABA_AR Mobility and Clustering during Plasticity

Fumihiro Niwa^{1,2}, Hiroko Bannai^{1*}, Misa Arizono^{1,3}, Kazumi Fukatsu¹, Antoine Triller⁴, Katsuhiko Mikoshiba¹

1 Laboratory for Developmental Neurobiology, Brain Science Institute (BSI), RIKEN, Saitama, Japan, **2** Laboratory of Functional Genomics, Department of Medical Genome Science, Graduate School of Frontier Science, The Institute of Medical Science, The University of Tokyo, Minato-ku, Tokyo, Japan, **3** Division of Neuronal Network, The Institute of Medical Science, The University of Tokyo, Tokyo, Japan, **4** Institut de Biologie de l'École Normale Supérieure (IBENS), Institut National de la Santé et de la Recherche Médicale U1024, Centre National de la Recherche Scientifique UMR8197, Paris, France

Abstract

The activity-dependent modulation of GABA-A receptor (GABA_AR) clustering at synapses controls inhibitory synaptic transmission. Several lines of evidence suggest that gephyrin, an inhibitory synaptic scaffold protein, is a critical factor in the regulation of GABA_AR clustering during inhibitory synaptic plasticity induced by neuronal excitation. In this study, we tested this hypothesis by studying relative gephyrin dynamics and GABA_AR declustering during excitatory activity. Surprisingly, we found that gephyrin dispersal is not essential for GABA_AR declustering during excitatory activity. In cultured hippocampal neurons, quantitative immunocytochemistry showed that the dispersal of synaptic GABA_ARs accompanied with neuronal excitation evoked by 4-aminopyridine (4AP) or *N*-methyl-D-aspartic acid (NMDA) precedes that of gephyrin. Single-particle tracking of quantum dot labeled-GABA_ARs revealed that excitation-induced enhancement of GABA_AR lateral mobility also occurred before the shrinkage of gephyrin clusters. Physical inhibition of GABA_AR lateral diffusion on the cell surface and inhibition of a Ca²⁺ dependent phosphatase, calcineurin, completely eliminated the 4AP-induced decrease in gephyrin cluster size, but not the NMDA-induced decrease in cluster size, suggesting the existence of two different mechanisms of gephyrin declustering during activity-dependent plasticity, a GABA_AR-dependent regulatory mechanism and a GABA_AR-independent one. Our results also indicate that GABA_AR mobility and clustering after sustained excitatory activity is independent of gephyrin.

Citation: Niwa F, Bannai H, Arizono M, Fukatsu K, Triller A, et al. (2012) Gephyrin-Independent GABA_AR Mobility and Clustering during Plasticity. PLoS ONE 7(4): e36148. doi:10.1371/journal.pone.0036148

Editor: Laurent Groc, Institute for Interdisciplinary Neuroscience, France

Received: December 16, 2011; **Accepted:** March 27, 2012; **Published:** April 26, 2012

Copyright: © 2012 Niwa et al. This is an open-access article distributed under the terms of the Creative Commons Attribution License, which permits unrestricted use, distribution, and reproduction in any medium, provided the original author and source are credited.

Funding: This work is supported by Grant-in-Aid for Scientific Research (20220007 to KM, 20700300 to HB), grants from the Kato Memorial Bioscience Foundation, and Toray Science Foundation (to HB). FN and MA were supported by the Junior Research Associate program of RIKEN. The funders had no role in study design, data collection and analysis, decision to publish, or preparation of the manuscript.

Competing Interests: The authors have declared that no competing interests exist.

* E-mail: hbannai@brain.riken.jp

Introduction

Inhibitory neurotransmission plays a critical role in the regulation of neuronal excitability and information processing in the brain. GABA-A receptors (GABA_ARs) are neurotransmitter receptors that mediate fast inhibitory neurotransmission in the central nervous system [1]. The number of GABA_ARs at the synapse is a factor that controls the efficacy of GABAergic transmission [2,3]. The number of synaptic GABA_ARs can be altered within a few minutes depending on neuronal inputs in the hippocampus. A brief application of *N*-methyl-D-aspartic acid (NMDA), which induces a chemical form of long-term depression at excitatory synapses, results in elevated inhibitory synaptic transmission through the increase of surface GABA_AR expression and synaptic accumulation of GABA_ARs [4,5]. By contrast, the decrease in the number of functional postsynaptic GABA_ARs and GABAergic synaptic currents is induced by brief high-frequency stimulation of Schaffer collateral fibers that produce long-term potentiation of excitatory synaptic transmission or induction of status epilepticus [6,7,8,9,10]. The latter process, i.e., activity-dependent reduction in the number of synaptic GABA_ARs, is mediated by the increase in intracellular Ca²⁺ concentration

followed by the activation of a Ca²⁺/calmodulin-activated phosphatase, calcineurin [7,10]. Several lines of evidence have indicated that calcineurin modulates the number of synaptic GABA_ARs by regulating their lateral mobility through the dephosphorylation of Ser327 in the GABA_AR γ 2 subunit [11,12,13]. However, the detailed molecular mechanism underlying the activity-dependent change in postsynaptic GABA_AR number remains unclear.

The interaction between neurotransmitter receptors and postsynaptic density proteins is an important factor that determines synaptic receptor number and density [14,15]. Gephyrin is a scaffold protein that directly binds to the α 1- α 3 subunit of GABA_ARs [16,17,18] and multiple proteins including tubulin, forming clusters at the GABAergic synapse [19]. Gephyrin plays a critical role in the regulation of synaptic GABA_AR stability because gene knockout, RNAi knockdown, and prevention of GABA_AR-gephyrin interaction result in a decrease in the number and density of synaptic GABA_ARs and an increase in GABA_AR mobility on the cell surface [16,20,21]. On the other hand, the formation and maintenance of synaptic gephyrin clusters also require synaptic localization of GABA_ARs [13,22,23,24,25,26,27].

A previous study revealed that the amount of postsynaptic gephyrin decreases when the number of synaptic GABA_ARs decreases as a result of excitatory activity [11]. In the present study, we tested the hypothesis that gephyrin declustering could be the starting point of this activity-induced regulation of GABA_AR lateral mobility and the number of postsynaptic GABA_ARs. Contrary to this hypothesis, we found evidence suggesting that excitatory activity impacts clustering of GABA_ARs first and gephyrin later.

Results

Activity-dependent decrease in synaptic GABA_ARs precedes that in gephyrin

We have previously shown the decrease in synaptic GABA_ARs and gephyrin when excitatory activity is increased [11]. To examine the timing of this process, we tracked changes in the immunofluorescence of synaptic GABA_AR, gephyrin, and the presynaptic marker protein synapsin after pharmacological neuronal stimulation every 2.5 min in cultured rat hippocampal neurons. For GABA_AR labeling, we developed a custom-made antibody that recognizes the extracellular domain of rat GABA_AR (amino acids 39–67). We confirmed that this antibody specifically recognized mouse GABA_AR $\gamma 2$ subunits expressed in HeLa cells (Fig. S1A–C). The antibody labeled clusters on the dendrites and cell bodies of cultured hippocampal neurons (Fig. S1D), as visualized by immunocytochemical staining with the antibody against the GABA_AR $\gamma 2$ subunit (amino acids 39–53) used in a previous study [11] (Fig. S1E). We therefore concluded that the anti-GABA_AR $\gamma 2$ antibody selectively recognizes the rodent GABA_AR $\gamma 2$ subunit.

Excitatory neuronal activity was induced by incubating cells with the potassium channel blocker 4-aminopyridine (4AP; 50 μ M) for 2.5, 5, 7.5, and 10 min before fixation. Treatment with 4AP did not affect the immunofluorescent intensity of synapsin (Fig. 1A and D), suggesting that the increase in neuronal activity has only a minor effect on the size of presynaptic terminals. By contrast, the immunoreactivity associated with total (synaptic and extrasynaptic) GABA_ARs significantly decreased to 75.3% \pm 2.3% of non-treated control cells within 2.5 min of incubation with 4AP (0 vs. 2.5 min, $p < 0.005$, ANOVA; $p < 0.005$, Tukey's range test in ANOVA), and no further decrease was induced by longer incubation (2.5–10 min, $p > 0.05$, Tukey's range test in ANOVA; Fig. 1B and E). Total gephyrin immunoreactivity also decreased to 78.5% \pm 2.7% of control cells (0 vs. 2.5 min, $p < 0.005$, Tukey's range test in ANOVA) within 2.5 min. However, we observed a further decrease of gephyrin immunoreactivity to 63.9% \pm 1.6% after incubation with 4AP for 7.5 min (2.5 vs. 7.5 min, $p < 0.005$, Tukey's range test in ANOVA; Fig. 1C and F). Synaptic GABA_AR and gephyrin clusters exhibited a time course similar to that of total GABA_AR and gephyrin clusters (Fig. 1G and H). These results indicated that the activity-dependent decrease in the number of synaptic GABA_AR clusters reached a steady state more quickly than that of synaptic gephyrin clusters.

Furthermore, we investigated the time courses of GABA_AR- and gephyrin-associated immunofluorescence recovery after washout of 4AP (Fig. S2A–C). Both synaptic GABA_AR and gephyrin immunoreactivity gradually recovered to almost the same level as that of non-treated cells within 10 min with a similar time course (Fig. S2E and F). No significant change in the size of the presynaptic terminals was detected by synapsin-associated immunofluorescence during the washout (Fig. S2D).

The comparison of the time courses of GABA_AR and gephyrin clusters raised the possibility that the excitatory activity-induced reduction in GABA_AR immunofluorescence precedes that in gephyrin immunofluorescence. Therefore, we further examined the 4AP-induced changes in GABA_AR- and gephyrin-associated immunoreactivity within 2.5 min (150 s). Stimulation by 4AP for 60 s induced the reduction in synaptic GABA_AR immunoreactivity to 73.0% \pm 2.5% of control cells ($p < 0.005$, Welch's *t*-test; Fig. 2A). However, synaptic gephyrin-associated immunofluorescence in the cells stimulated by 4AP for 60 s maintained the same intensity as observed in 4AP non-treated cells (106.6% \pm 3.8% of control cells, $p > 0.05$, Welch's *t*-test; Fig. 2B). We then examined the timing of NMDA-induced changes in GABA_AR- and gephyrin-associated immunoreactivities, as the activation of the NMDA receptor and subsequent Ca²⁺ influx is also involved in the neuronal excitatory activity-dependent decrease in GABAergic synaptic transmission and declustering of GABA_ARs at inhibitory synapses [7,12,28]. When neurons were stimulated by 50 μ M NMDA with its co-agonist, glycine, and TTX for 60 s, synaptic GABA_AR immunoreactivity declined to 76.1% \pm 2.3% of control cells ($p < 0.005$, Welch's *t*-test; Fig. 2C). By contrast, synaptic gephyrin-associated immunofluorescence was unaffected by NMDA stimulation for 60 s (96.8% \pm 4.7% of control cells, $p > 0.05$, Welch's *t*-test; Fig. 2D). Longer NMDA treatment (150 s) resulted in the reduction of synaptic gephyrin immunoreactivity, as similarly observed with 4AP treatment; synaptic gephyrin immunoreactivity was reduced to 77.9% \pm 2.2% of control cells ($p < 0.005$, Welch's *t*-test; Fig. 2E). These results, together with the results of the time-course analysis of 4AP treatment, indicate that the excitatory activity-induced decrease in the number of synaptic GABA_ARs at postsynapses takes place before the shrinkage of synaptic gephyrin clusters.

Modulation of GABA_AR diffusion is complete before that of gephyrin clustering

The increase in GABA_AR lateral diffusion dynamics plays a key role in neuronal activity-dependent decrease in GABA_AR clustering at inhibitory synapses [11,12]. Therefore, we conducted a time-course analysis of GABA_AR lateral diffusion dynamics after 4AP stimulation using single-particle tracking with quantum dots (QD-SPT) [29]. Endogenous GABA_ARs were targeted with an antibody against the extracellular domain of the $\gamma 2$ subunit (Fig. S1D) and subsequently labeled with an intermediate biotinylated Fab fragment and streptavidin-coated QDs. The lateral diffusion parameters after 4AP stimulation were calculated from the trajectories of GABA_ARs labeled with QDs (GABA_AR-QDs) (Fig. 3A). The location of the active synapse was visualized by labeling with the amphiphilic dye FM4–64, induced after a burst of activity with 40 mM KCl. We confirmed that this FM4–64 labeling did not affect the GABA_AR diffusion coefficient both in the absence and presence of 4AP treatment (Fig. S3A). The diffusion coefficient of GABA_AR-QD at the synapse obtained by synaptic trajectories (red in Fig. 3A) was significantly increased within 2.5 min after the onset of 4AP stimulation (0–10 min, $p < 0.005$, Kruskal–Wallis test; 0 vs. 2.5 min, $p < 0.005$, Mann–Whitney *U* test; Fig. 3B and C). An additional increase in diffusion coefficient was not induced by longer incubation (2.5–10 min, $p > 0.05$, Kruskal–Wallis test). In the absence of FM4–64 labeling, a 4AP-induced increase in diffusion coefficient was observed within 4 min (Fig. S3B), suggesting that the KCl-induced burst during FM4–64 labeling does not significantly impact the time course of 4AP-induced changes in the GABA_AR diffusion coefficient. Forty to fifty percent of synaptic GABA_AR-QD exhibited “confined diffusion,” i.e., lateral diffusion limited to a

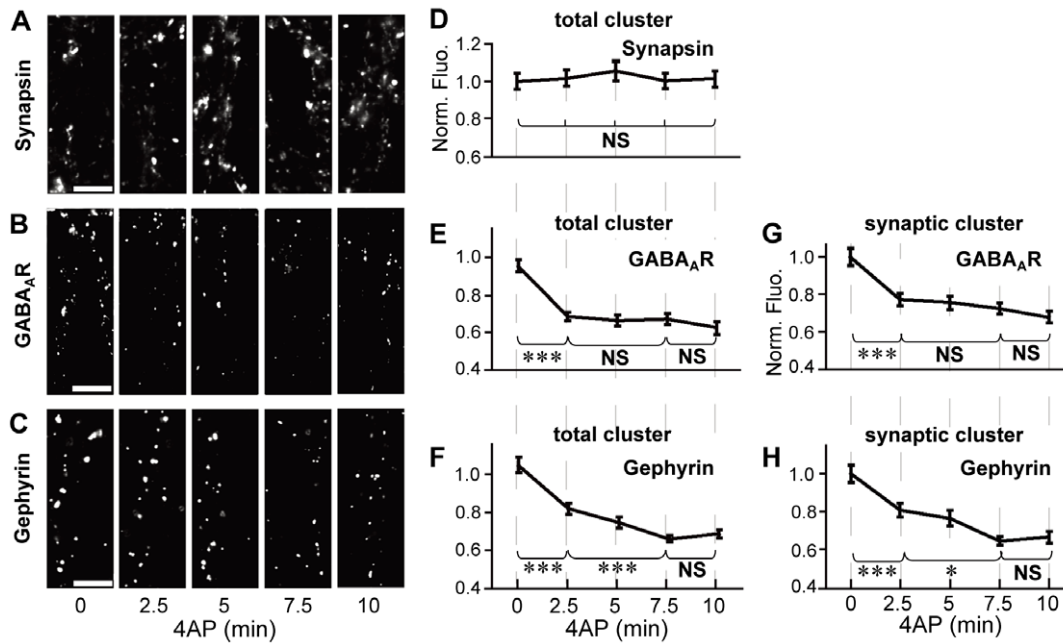


Figure 1. Time-course analysis of 4AP-induced decrease in GABA_AR- and gephyrin-associated immunofluorescence. A–C: Representative examples of immunoreactivity associated with synapsin (A), GABA_AR (B), and gephyrin (C) on the dendrites of hippocampal neurons (21–27 DIV) treated with 50 μ M 4AP for 0–10 min. Scale bars: 5 μ m. D–F: Time-course plots of changes in normalized fluorescence intensities (averages \pm SEM) of total clusters of synapsin (D), GABA_AR (E), and gephyrin (F) following 4AP treatment. G, H: Time-course plots of 4AP-induced reduction in the normalized fluorescence intensities of synaptic GABA_AR (G) and gephyrin (H) clusters. NS: $p > 0.05$, *: $p < 0.05$, ***: $p < 0.005$, Tukey's range test in ANOVA, $n = 40$ cells/condition (4 cultures). doi:10.1371/journal.pone.0036148.g001

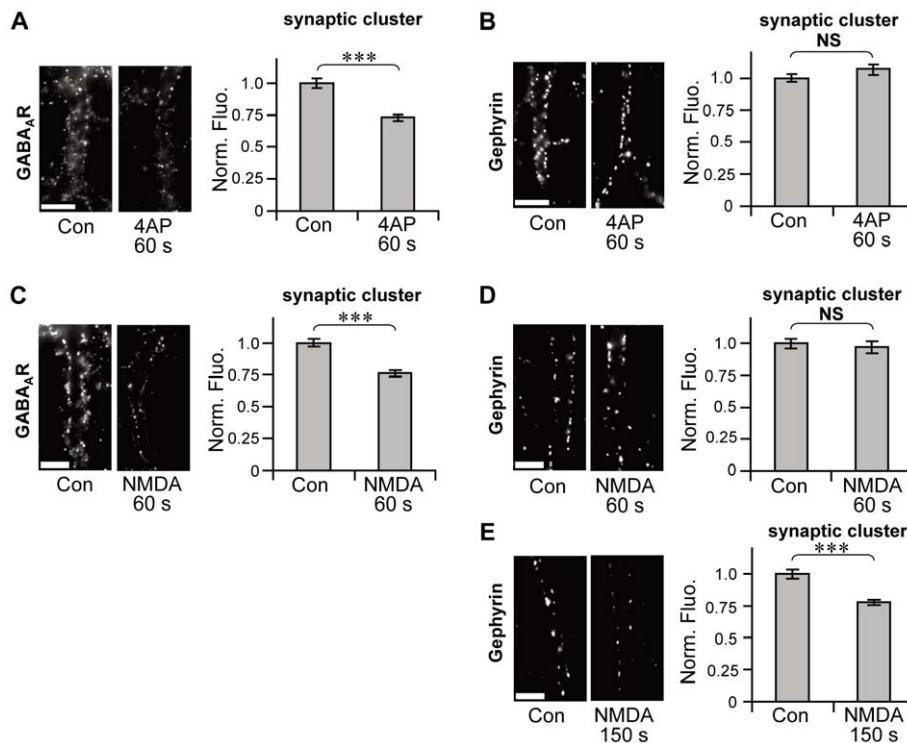


Figure 2. Activity-dependent decrease in synaptic clusters of GABA_AR preceding that of gephyrin. Left: Representative examples of immunoreactivity associated with GABA_AR (A, C) and gephyrin (B, D, E) in the presence (A, B: 4AP, C–E: NMDA) or absence (Con) of stimulation for the indicated times. Right: Normalized fluorescence intensities (averages \pm SEM) of synaptic GABA_AR (A, C) and gephyrin (B, D, E) clusters following stimulation. Note that fluorescence intensity of gephyrin was unchanged 60 s after the onset of stimulation (4AP: B, NMDA: D), while that of GABA_AR significantly decreased at 60 s (4AP: A, NMDA: C). Scale bars: 5 μ m. NS: $p > 0.05$, ***: $p < 0.005$, Welch's t -test, $n = 30$ cells/condition (3 cultures). doi:10.1371/journal.pone.0036148.g002

small surface area [30], as reported previously [11]. The size of confinement was calculated for this population (see Materials and Methods). The average confinement size was significantly increased to $131.4\% \pm 6.9\%$ of control cells by 4AP treatment for 2.5 min (0 vs. 2.5 min, $p < 0.005$, Tukey's range test in ANOVA) and then maintained during further incubation (2.5–10 min, $p > 0.05$, Tukey's range test in ANOVA; Fig. 3D). Furthermore, the synaptic dwell time of GABA_AR-QD decreased to $73.8\% \pm 3.8\%$ of control cells at 2.5 min (0 vs. 2.5 min, $p < 0.005$, Tukey's range test in ANOVA); however, no further decrease was observed after 2.5 min (2.5–10 min, $p > 0.05$, Tukey's range test in ANOVA) (Fig. 3E). These results indicate that 4AP-dependent modification of GABA_AR lateral diffusion reaches a steady state within 2.5 min, which probably leads to the decrease in the number of synaptic GABA_ARs (Fig. 1G). The time taken by gephyrin-associated immunofluorescence to reach a steady state was 7.5 min (Fig. 1H). This is 5 min longer than the time taken for GABA_AR diffusion dynamics to reach a steady state. Therefore, our results indicate that the activity-dependent change in the lateral diffusion of GABA_ARs is completed before the dispersion of gephyrin clusters.

4AP-dependent modulation of gephyrin clusters depends on GABA_AR lateral mobility

It is well established that synaptic gephyrin clustering also requires synaptic localization of GABA_ARs [13,22,23,24,25,26,27]. Based on the finding that the excitatory activity-induced modulation of GABA_AR lateral diffusion was accomplished before gephyrin declustering, we hypothesized that gephyrin clustering could be sensitive to GABA_AR diffusion dynamics, in addition to its existence and localization. To confirm this hypothesis, we manipulated GABA_AR diffusion dynamics by artificially cross-linking (XL) the GABA_AR $\gamma 2$ subunits using antibodies, as performed previously for AMPA receptors and metabotropic glutamate receptors [31,32]. Successful XL of GABA_ARs was confirmed by the appearance of fluorescent clusters labeled with the Alexa Fluor[®]-conjugated antibody used for XL of primary antibodies targeted to GABA_ARs (Fig. 4A). The fluorescence intensities of these cross-linked GABA_AR clusters were not affected by 4AP treatment (Fig. 4B). Next GABA_AR mobility was examined by QD-SPT. Trajectories revealed that the area explored by GABA_AR-QDs were greatly reduced when surface GABA_ARs were cross-linked, both inside (red, Fig. 4C) and outside (blue, Fig. 4C) the synapses. In the absence of 4AP, XL induced an approximately 100-fold reduction in GABA_AR-QD diffusion coefficients (Fig. 4D), an approximately 3.7-fold increase in the percentage of immobilized GABA_AR-QD (Fig. 4E), a 13.6% decrease in the confinement size (Fig. 4F), and an approximately 3.4-fold increase in the synaptic dwell time (Fig. 4G), indicating that GABA_AR-QD lateral diffusion is greatly inhibited by XL. Moreover, XL blocked the 4AP-induced significant increase in the diffusion coefficient, enlargement of confinement size, and decrease in the synaptic dwell time of GABA_AR-QDs (Fig. 4D–G).

We also confirmed that 4AP-induced increase in intracellular Ca²⁺ remained unaffected under XL conditions, which is responsible for the increase in GABA_AR lateral diffusion. Ca²⁺ imaging with fluo-4 at proximal dendrites revealed that increase in intracellular Ca²⁺ was successfully induced by 4AP treatment even under XL conditions (Fig. 5B) as observed in the absence of XL (Fig. 5A), and that there was no significant difference in the peak amplitudes (Fig. 5C) and levels of increase in intracellular Ca²⁺ as represented by the area under the curve (Fig. 5D) between control and XL cells. Taken together, these experiments indicate that XL could inhibit GABA_AR lateral diffusion without affecting intra-

cellular Ca²⁺ elevation. Next we examined 4AP-induced declustering of gephyrin under XL conditions (Fig. 5E). Although a previous study showed that a 12-h XL of GABA_AR resulted in the formation of extrasynaptic gephyrin clusters [33], the total number of gephyrin clusters in GABA_AR XL conditions was not different from that without XL (Fig. 5F), suggesting that extrasynaptic artificial gephyrin clusters are not formed under our XL conditions. In the cells without GABA_AR XL, 4AP incubation for 15 min significantly decreased gephyrin-associated immunoreactivity [Fig. 5G (–XL)]. Conversely, the same 4AP stimulation failed to induce reduction in gephyrin immunofluorescence in the cells with GABA_AR XL [Fig. 5G (+XL)].

XL of surface GABA_ARs is an extreme condition in which a large proportion of surface GABA_ARs are immobilized. Therefore, we also examined the effect of a calcineurin inhibitor, cyclosporin A (CysA), which does not immobilize surface GABA_ARs but suppresses the NMDA-induced increase in GABA_AR mobility [11,12], on gephyrin clustering. We confirmed that the 4AP-driven increase in the synaptic diffusion coefficient (Fig. 6A) and reduction in the synaptic dwell time (Fig. 6B) were completely inhibited in the presence of 1 μ M CysA (Fig. 6C and D), which is in agreement with previous studies of NMDA stimulation [11,12]. Ca²⁺ imaging with fluo-4 revealed that increase in intracellular Ca²⁺, sustained for at least 15 min, was normally induced by 4AP even in the presence of CysA (Fig. 6E). The peak amplitude (Fig. 6F) and Ca²⁺ influx level represented by the area under the curve (Fig. 6G) was not significantly affected by CysA ($p > 0.05$, Welch's *t*-test). Under this condition, the size of synaptic clusters of GABA_AR and gephyrin was quantified by immunocytochemistry. The shrinkage of synaptic GABA_AR clusters induced by 4AP stimulation for 30 min (Fig. 6H) was blocked completely in the presence of CysA (Fig. 6I). Furthermore, 4AP-driven gephyrin declustering at the synapse (Fig. 6J) was also prevented by CysA treatment (Fig. 6K), despite the increase in cytosolic Ca²⁺.

In summary, the above results indicate that 4AP-driven gephyrin declustering is inhibited when there is no increase in GABA_AR lateral diffusion in response to neuronal excitation. Our results also imply that synaptic gephyrin clustering is dependent on the mobility of GABA_ARs during sustained activity induced by 4AP.

NMDA-driven gephyrin declustering is independent of GABA_AR mobility

The result of GABA_AR XL and CysA experiments with 4AP stimulation suggested the existence of a mechanism, dependent on GABA_AR surface mobility, which regulates gephyrin clustering. Finally, we examined whether gephyrin clustering is constantly subjected to this GABA_AR-dependent regulation during sustained neuronal excitation. NMDA stimulation was applied to increase neuronal activity, and effects of CysA treatment on synaptic GABA_AR and gephyrin clusters were examined. In agreement with previous reports that CysA inhibits NMDA-induced increase in GABA_AR lateral diffusion [11,12] and declustering of GABA_ARs [12], the dispersal of synaptic GABA_AR observed after 30 min of NMDA treatment (Fig. 7A) was completely blocked by the presence of CysA (Fig. 7B). NMDA stimulation significantly diminished the size of gephyrin clusters to $26.7\% \pm 0.9\%$ of control cells (Fig. 7C). Unlike the GABA_AR clusters, synaptic gephyrin clusters were reduced ($31.0\% \pm 2.1\%$ of control cells, Fig. 7D) even in the presence of CysA. XL of surface GABA_ARs also failed to inhibit NMDA-induced declustering of gephyrin (Fig. 7E). Interestingly, increase in Ca²⁺ induced by NMDA stimulation, which persisted for at least 15 min, was larger than that induced by 4AP

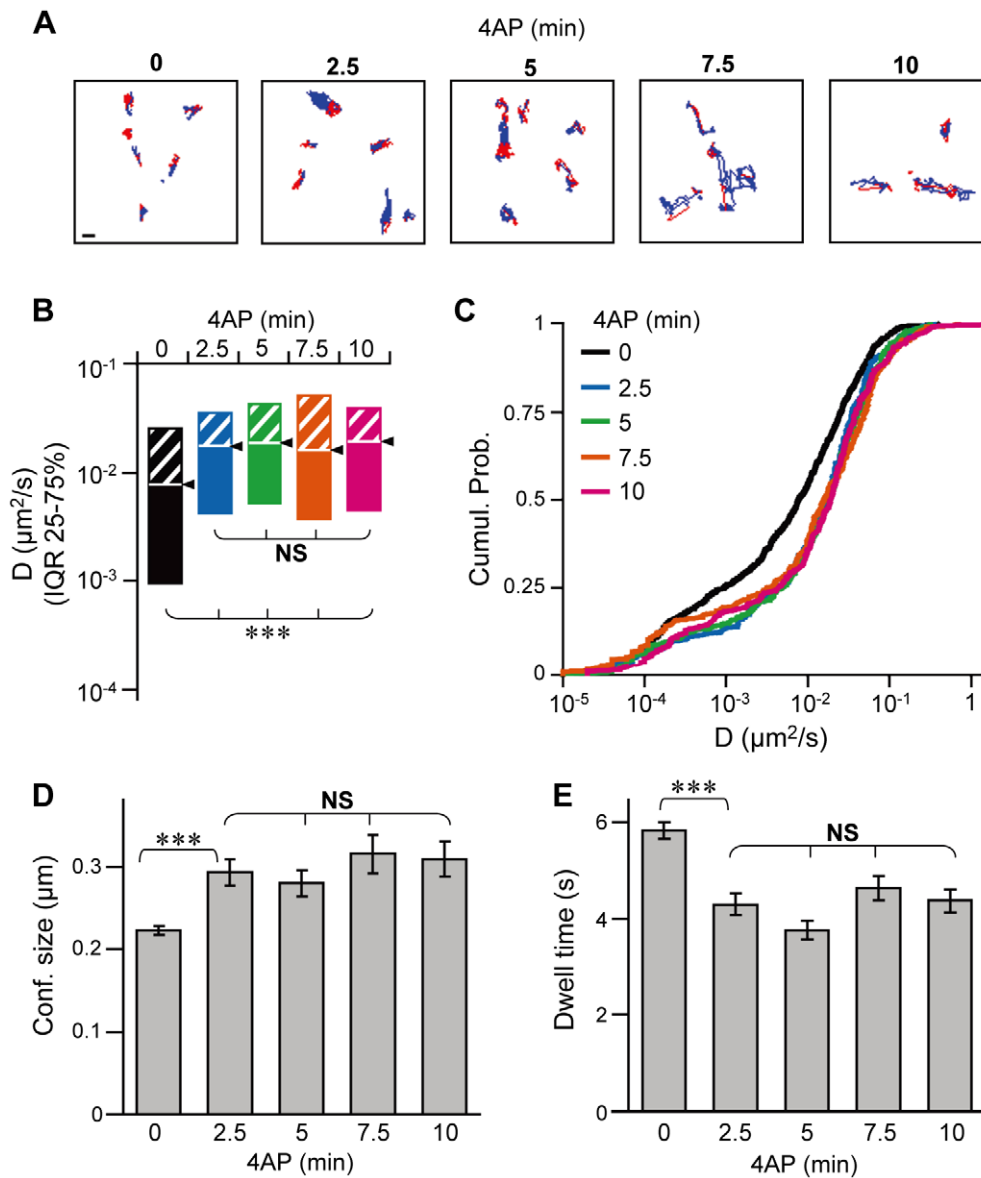


Figure 3. Modulation of GABA_AR lateral diffusion by 4AP completed within 2.5 min. **A:** Examples of trajectories of GABA_AR-QDs recorded for 38.9 s in neurons treated for the indicated times with 4AP, inside (red) and outside (blue) the synapse. Scale bar: 1 μm. **B, C:** The diffusion coefficients (D) of GABA_AR-QDs inside the synapses in neurons incubated with 4AP for 0–2.5 min (2.5 min), 2.5–5 min (5 min), 5–7.5 min (7.5 min), and 7.5–10 min (10 min) and that in control cells (0 min). Median diffusion coefficients (triangle) and plus (hatched) and minus (solid) interquartile ranges (IQR) (**B**) and cumulative probability (**C**) of the synaptic diffusion coefficients of GABA_AR-QDs. 0 min: n=974 QDs; 2.5 min: n=290; 5 min: n=295; 7.5 min: n=258; 10 min: n=258. ***: $p < 0.005$, NS: $p > 0.05$, Kruskal–Wallis test. **D:** The average (\pm SEM) confinement sizes of GABA_AR-QDs in synapses. 0 min: n=500 QDs; 2.5 min: n=122; 5 min: n=106; 7.5 min: n=127; 10 min: n=111. **E:** The average synaptic dwell times (\pm SEM) of GABA_AR-QD. 0 min: n=3466 events; 2.5 min: n=1147; 5 min: n=1320; 7.5 min: n=1131; 10 min: n=1098. NS: $p > 0.05$, ***: $p < 0.005$, Tukey's range test in ANOVA (**D, E**). Data were obtained from 3 or 4 cultures. doi:10.1371/journal.pone.0036148.g003

(Fig. 7F). The average peak amplitude of Ca²⁺ elevation evoked by NMDA was 1.2 times larger than that induced by 4AP ($p < 0.005$, Welch's *t*-test; Fig. 7G) and the level of increase in Ca²⁺ during NMDA stimulation was 1.3 times higher than that during 4AP stimulation ($p < 0.005$, Welch's *t*-test; Fig. 7H). Taken together, these results suggest that gephyrin clustering is not dependent on GABA_AR mobility during sustained activity induced by NMDA, possibly at high levels of increase in Ca²⁺. More importantly, despite the loss of synaptic gephyrin clustering by NMDA stimulation (Fig. 7D), Cys A blocked NMDA-induced declustering of GABA_ARs (Fig. 7B) and the increase in lateral diffusion [11,12].

These results clearly indicate that lateral diffusion of GABA_ARs at the synapse and synaptic GABA_AR clustering during inhibitory synaptic plasticity are independent of the amount of synaptic gephyrin present.

Discussion

The main finding of this study is that changes in lateral diffusion dynamics and number of synaptic GABA_ARs preceded gephyrin declustering during excitatory activity. In addition, our results indicate that synaptic GABA_AR diffusion and clustering are

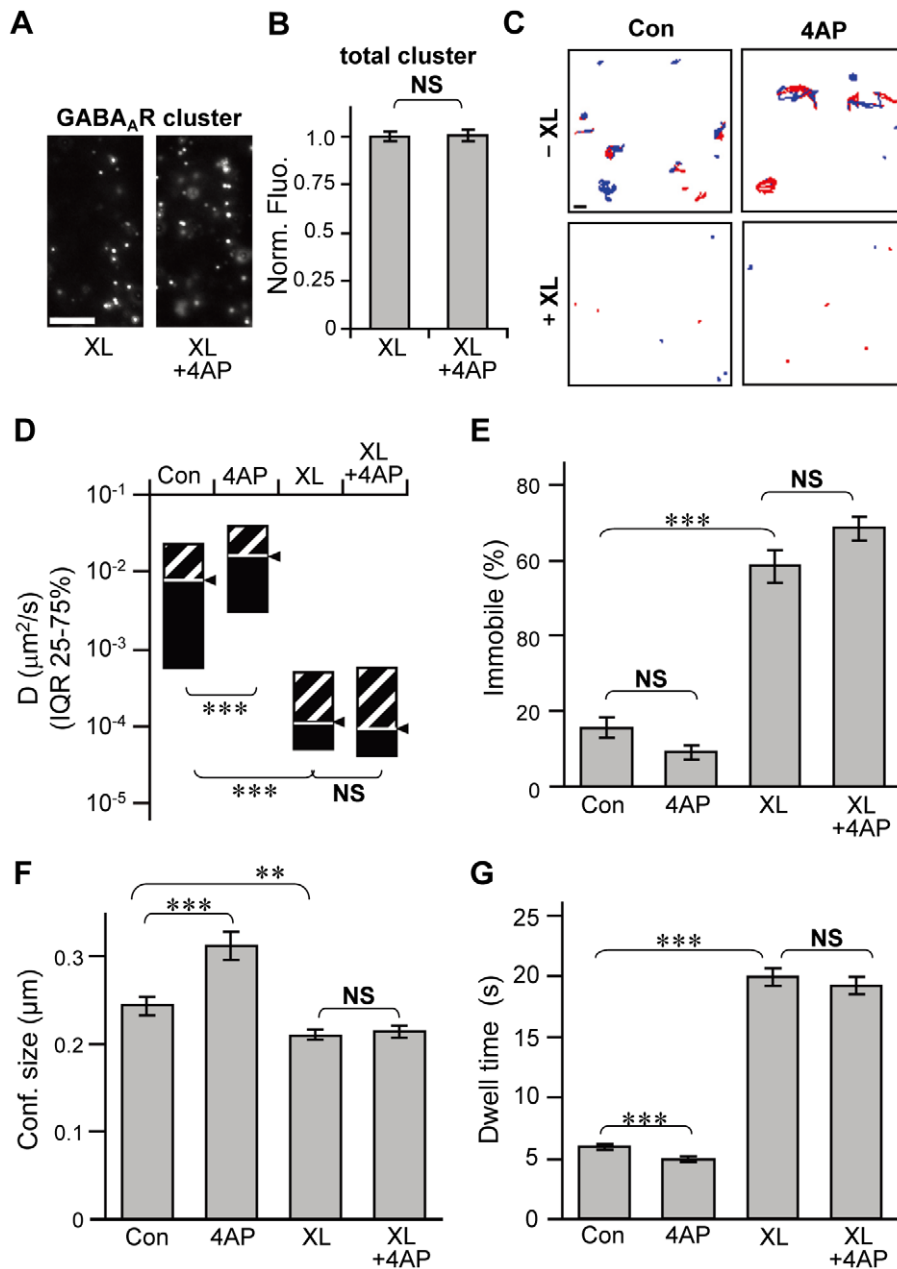


Figure 4. Inhibition of GABA_AR lateral diffusion by cross-linking (XL). **A:** Examples of cross-linked GABA_AR clusters on the dendrites of hippocampal neurons with (XL+4AP) or without (XL) 4AP stimulation. Scale bar: 5 μm. **B:** Normalized average fluorescent intensities of cross-linked GABA_AR clusters with (XL+4AP) or without (XL) 4AP stimulation (averages ± SEM). XL: n=39 cells; XL+4AP: n=40 cells, from 4 cultures. **C:** Representative trajectories of GABA_AR-QDs recorded for 38.9 s with (+XL) or without (-XL) XL in the presence or absence of 4AP, inside (red) and outside (blue) the synapse. Scale bar: 1 μm. **D–G:** Effects of XL and 4AP treatment on diffusion coefficients (**D**), percentage of immobile receptors (**E**), synaptic confinement sizes (**F**), and synaptic dwell times (**G**) of GABA_AR-QDs. **D:** The diffusion coefficients of GABA_AR-QDs (median ± IQR). The number of GABA_AR-QDs analyzed: Con: n=556; 4AP: n=418; XL: n=321; XL+4AP: n=321. **E:** The percentage of immobile GABA_AR-QDs (average ± SEM). Con: n=15 cells; 4AP: n=14; XL: n=14; XL+4AP: n=19. **F:** The confinement size (average ± SEM) of synaptic GABA_AR-QDs. Con: n=366 QDs; 4AP: n=203; XL: n=200; XL+4AP: n=196. **G:** The average dwell times (±SEM) of GABA_AR-QDs in synapses. Con: n=2039 events; 4AP: n=1576; XL: n=473; XL+4AP: n=493. Data in **D–G** were obtained from 3 cultures. NS: *p*>0.05, **: *p*<0.01, ***: *p*<0.005, Welch's *t*-test for **B**, **E–G**, and Mann-Whitney *U* test for **D**. doi:10.1371/journal.pone.0036148.g004

independent of the status of gephyrin clusters during sustained excitatory activity.

Gephyrin is considered a key protein that controls GABA_AR stability at the postsynapse [13,16,20,21]. In this study, we tested the hypothesis that the excitatory activity-dependent reduction in postsynaptic GABA_AR [11,12], which could be involved in

GABAergic synaptic plasticity, is initiated by the dispersion of gephyrin from clusters. If this hypothesis were correct, excitatory activity should have affected gephyrin first or at least at the same time when affecting GABA_AR. Contrary to this expectation, a detailed time-course analysis indicated that the dispersal of GABA_AR clusters induced by the enhancement of GABA_AR

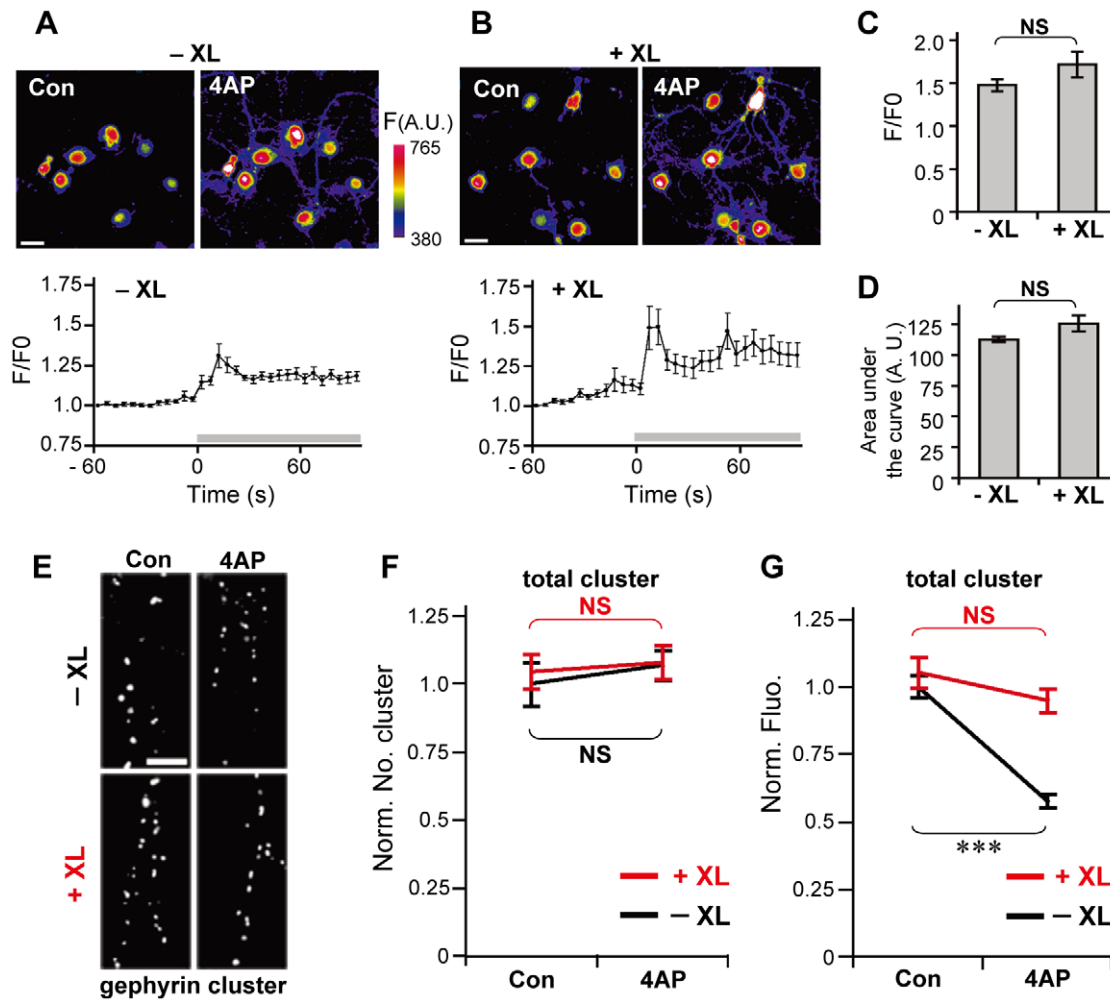


Figure 5. Suppression of 4AP-induced reduction in gephyrin immunofluorescence by GABA_AR immobilization under increased levels of cytosolic Ca²⁺. **A, B:** Top: Representative pseudocolor images of hippocampal neurons loaded with fluo-4 AM without (**A**) or with (**B**) surface GABA_AR XL, before (Con) and 10 s after 4AP application (4AP). Scale bars: 20 μm. Bottom: Time-course plots of F/F₀ ratio changes (averages ± SEM) measured on proximal dendrites with the addition of 4AP, in the absence (**A**) or presence (**B**) of GABA_AR XL. 4AP was applied at time=0 as indicated by the gray horizontal bar in the traces. **C, D:** Peak amplitudes (**C**) and areas under the curve (**D**) for the F/F₀-time plot during 90 s after addition of 4AP. Values indicate averages ± SEM. NS: $p > 0.05$, Welch's *t*-test. -XL: $n = 30$ cells, +XL: $n = 28$, from 3 cultures. Note that normal increase in Ca²⁺ was induced by 4AP even under XL conditions. **E:** Examples of gephyrin-immunoreactive clusters in dendrites with (+XL) or without (-XL) surface GABA_AR XL in the presence (4AP) and absence (Con) of 4AP treatment for 10 min. Scale bar, 5 μm. **F, G:** Effects of GABA_AR XL and 4AP treatment on the normalized number of clusters (**F**) and normalized fluorescence intensities (**G**) of gephyrin clusters (averages ± SEM). NS: $p > 0.05$; ***: $p < 0.005$, Welch's *t*-test, $n = 30$ cells/condition (3 cultures). 4AP-induced reduction in gephyrin cluster size was completely suppressed by GABA_AR XL.

doi:10.1371/journal.pone.0036148.g005

lateral mobility preceded the dispersal of gephyrin. Our results suggest that neuronal activity-induced rapid decrease in GABA_AR numbers at mature inhibitory synapses is not mediated by gephyrin declustering. This notion was further supported by the observation that synaptic GABA_AR mobility and clustering were not affected by NMDA in the presence of CysA, while gephyrin cluster largely decreased under the same conditions. Our findings suggest that excitatory activity-induced plasticity in GABAergic synapses is induced independent of the status of gephyrin clusters.

There was no remarkable difference in the recovery time course of GABA_AR and gephyrin cluster size after 4AP removal, similar to the process of synaptogenesis in hippocampal neurons [34,35]. This suggests that the reaccumulation of GABA_AR and gephyrin to the inhibitory synapse occurs simultaneously. It remains unclear whether gephyrin is critical for the recovery of GABA_AR clusters.

Furthermore, our results suggested that there are existence two regulatory mechanisms of gephyrin clustering during sustained activity: GABA_AR-dependent and GABA_AR-independent mechanisms. The amount of gephyrin in clusters was maintained even in the presence of 4AP, when surface GABA_ARs were immobilized by XL and when 4AP-induced increase in GABA_AR diffusion was prevented by CysA-treatment. This finding indicates that GABA_AR lateral diffusion dynamics can affect clustering of the scaffold protein gephyrin. Recent theoretical modeling of postsynaptic structures based on chemical potential proposed another concept which states that the stabilization of the postsynaptic structure is reciprocal. In other words, scaffold proteins stabilize receptors and receptors stabilize scaffold proteins [36]. Together with the fact that gephyrin is crucial for the stabilization of postsynaptic GABA_ARs [16,20,21], our data provide direct evidence of a reciprocal mechanism that stabilizes

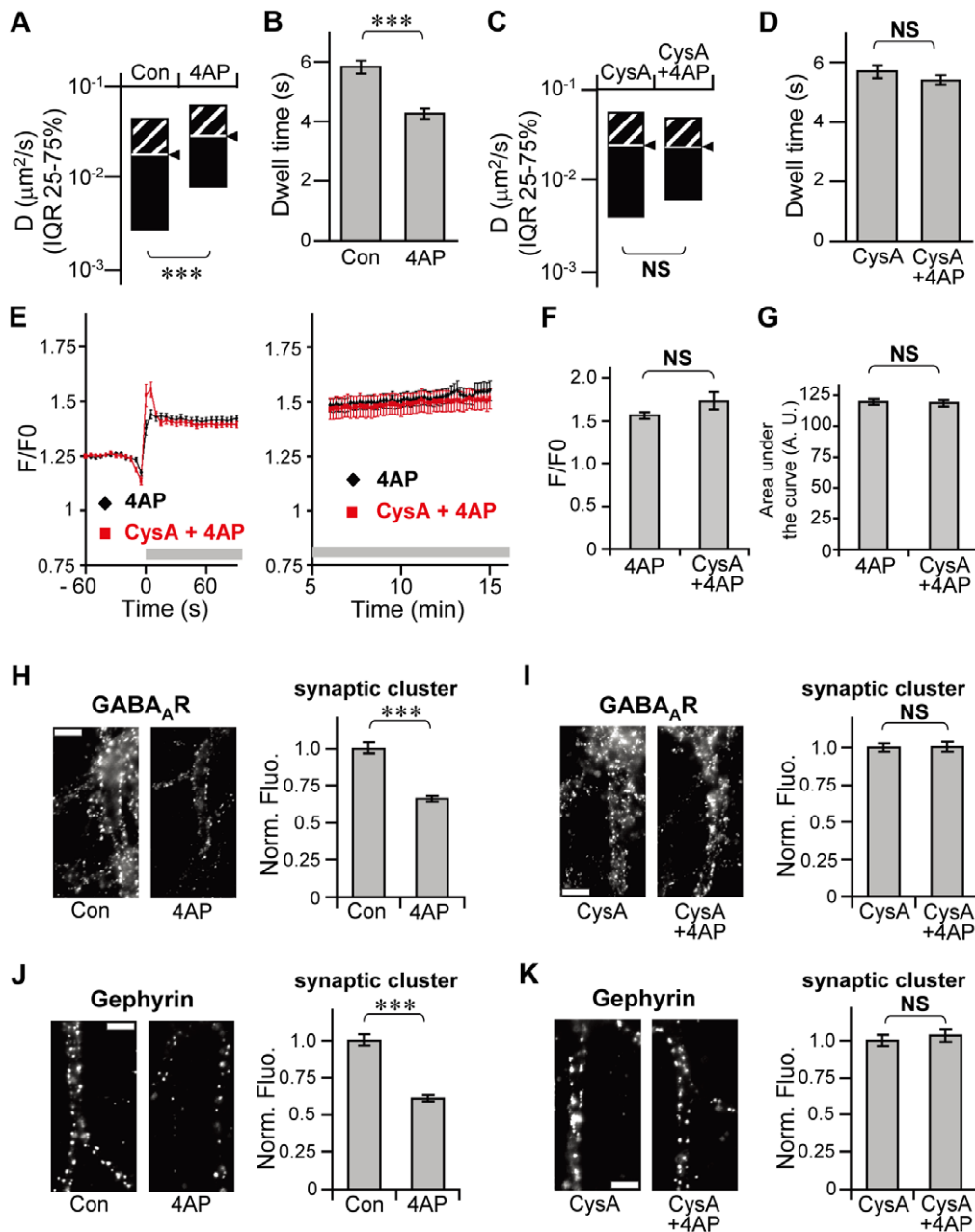


Figure 6. Prevention of 4AP-induced gephyrin declustering by calcineurin inhibitor CysA. **A–D:** Inhibition of 4AP-driven mobilization of GABA_AR-QDs by CysA treatment. Diffusion coefficients in the synapse (**A** and **C**, median \pm IQR) and synaptic dwell times (**B** and **D**, averages \pm SEM) in the absence (**A**, **B**) or presence (**C**, **D**) of 1 μM CysA. NS: $p > 0.05$, ***: $p < 0.005$, Mann–Whitney U test for **A**, **C** (Con: $n = 535$ QDs, 4AP: $n = 537$, CysA: $n = 478$, CysA+4AP: $n = 506$), Welch’s t -test for **B**, **D** (Con: $n = 2107$ events, 4AP: $n = 2505$, CysA: $n = 1930$, CysA+4AP: $n = 2094$). Data were obtained from 3 cultures. **E–G:** Intact 4AP-induced increase in cytosolic Ca^{2+} concentration under CysA treatment. Changes in intracellular Ca^{2+} levels indicated as F/F0 of fluo-4 after the addition of 4AP (black) or CysA+4AP (red) (**E**). Drugs, i.e. 4AP or CysA+4AP, were applied at time = 0 as indicated by the gray horizontal bar in the traces. Peak amplitudes of F/F0 (**F**) and areas under the F/F0-time curve (**G**) during 90 s after the onset of stimulation. Values indicate averages \pm SEM. NS: $p > 0.05$, Welch’s t -test. 4AP: $n = 26$ cells, CysA+4AP: $n = 28$ cells (3 cultures). **H–K:** The effect of CysA treatment on 4AP-driven declustering of GABA_AR and gephyrin. Left: Example of immunoreactivity associated with GABA_AR (**H**, **I**) and gephyrin (**J**, **K**) on the dendrites treated with 4AP for 30 min, in the absence (**H**, **J**) and presence (**I**, **K**) of CysA. Scale bars: 5 μm . Right: Normalized fluorescence intensities (averages \pm SEM) of synaptic GABA_AR (**H**, **I**) and gephyrin (**J**, **K**) clusters. NS: $p > 0.05$, ***: $p < 0.005$, Welch’s t -test. Con, CysA: $n = 30$ cells/condition, 4AP, CysA+4AP: $n = 25$ cells/condition from 3 cultures. doi:10.1371/journal.pone.0036148.g006

the structure of GABAergic synapses. Regulation of postsynaptic scaffolds by neurotransmitter receptors is involved in synaptogenesis and the maintenance of GABAergic synapses, as evidenced by the fact that the absence of some GABA_AR subunits results in the disappearance of gephyrin clusters [22,23,24,25,26,27]. Our

present results, which imply that activity-induced mobilization of surface GABA_ARs destabilizes gephyrin clusters, also raise the possibility that GABA_AR lateral mobility, in addition to its existence and localization, could be a primary determinant of stability of mature GABAergic synaptic structures during synaptic

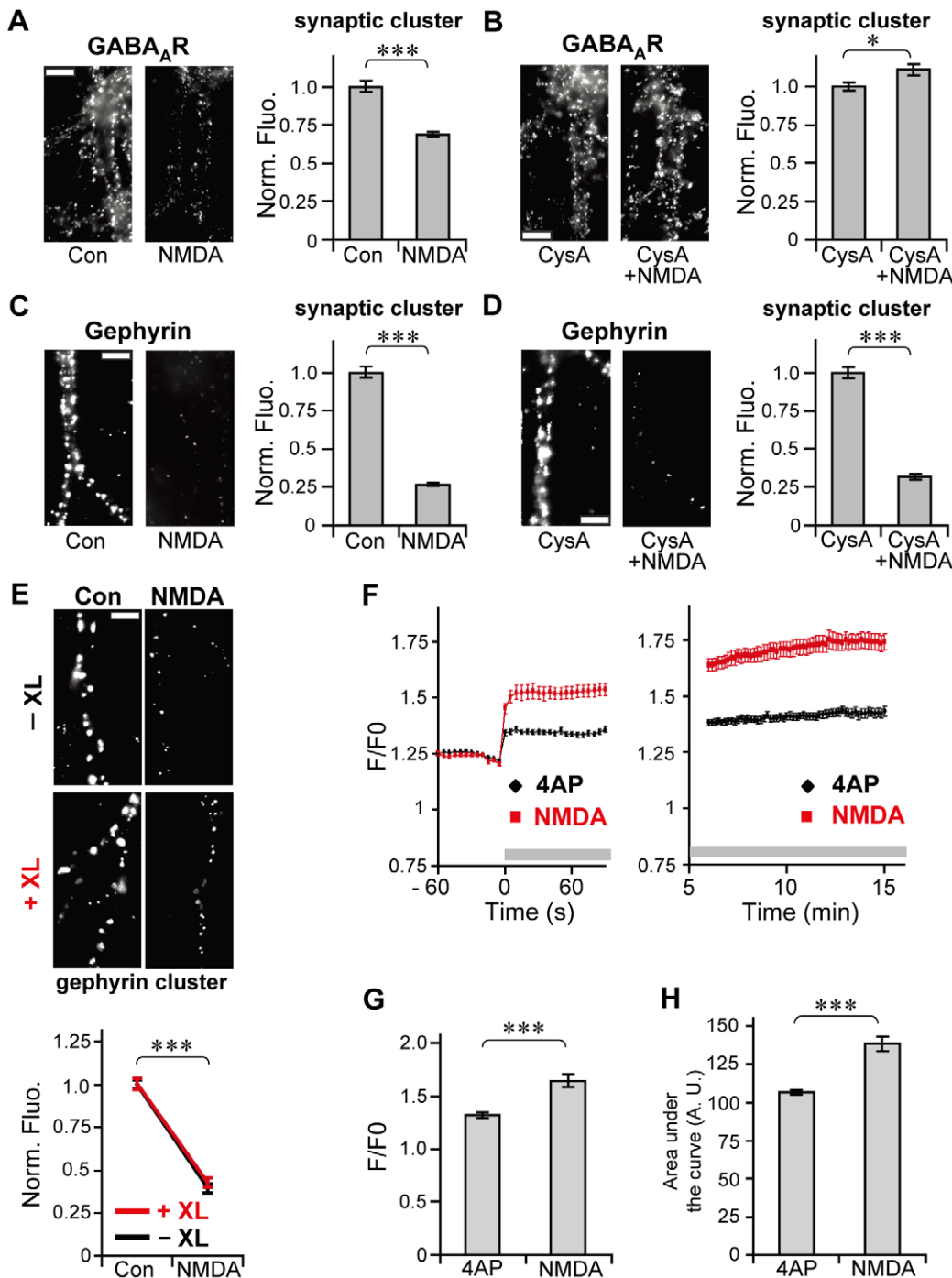


Figure 7. GABA_A-independent gephyrin declustering during sustained activity induced by NMDA stimulation. **A–D:** Effect of CysA treatment on NMDA-driven dispersal of GABA_AR and gephyrin clusters. Left: Examples of GABA_AR (**A**, **B**) and gephyrin (**C**, **D**) immunoreactivity in neurons incubated with NMDA for 30 min, with (**B**, **D**) and without CysA (**A**, **C**). Scale bars, 5 μ m. Right: Normalized fluorescence intensities (averages \pm SEM) of synaptic GABA_AR (**A**, **B**) and gephyrin (**C**, **D**) clusters. *: $p < 0.05$, ***: $p < 0.005$, Welch's t -test. Con, CysA, CysA+NMDA: $n = 30$ cells/condition, NMDA: $n = 25$ cells/condition (3 cultures). CysA suppressed NMDA-induced dispersal of GABA_AR clusters, but not that of gephyrin clusters. **E:** NMDA-induced gephyrin dispersal under GABA_AR XL. Top: Gephyrin immunoreactive clusters in neurons with (+XL) and without (–XL) surface GABA_AR XL after NMDA stimulation. Bottom: Effects of GABA_AR XL and NMDA treatment on the normalized fluorescence intensity of gephyrin clusters (average \pm SEM). ***: $p < 0.005$, Welch's t -test, $n = 30$ cells/condition (3 cultures). **F–H:** Comparison of the Ca²⁺ influx level induced by 4AP and NMDA. Increase in Ca²⁺ after the addition of 4AP (black) or NMDA (red) (**F**). Gray horizontal bars in the traces indicate the presence of 4AP or NMDA. Peak amplitudes (**G**) and areas under the curve (**H**) for F/F₀-time plots during 90 s after the onset of stimulation. Values indicate averages \pm SEM. ***: $p < 0.005$, Welch's t -test. 4AP: $n = 21$ cells, NMDA: $n = 23$ cells (3 cultures). doi:10.1371/journal.pone.0036148.g007

plasticity. Changes in the chemical potential associated with GABA_ARs and gephyrin, which are induced by the enhancement of lateral diffusion and subsequent decrease in synaptic GABA_AR density, could lead to a new steady state of postsynaptic molecular assembly [36].

The observation that gephyrin dispersed after NMDA stimulation regardless of GABA_AR mobility suggested that another GABA_AR-independent regulatory mechanism may control gephyrin clustering. Considering that NMDA induced a 1.3 times larger Ca²⁺ elevation than 4AP, the Ca²⁺ influx level could be one of the factors determining whether gephyrin is subjected to GABA_AR-dependent regulation or independently destabilized in response to Ca²⁺ elevation. Gephyrin is a substrate of the Ca²⁺-dependent non-lysosomal cysteine protease calpain-1, which is activated when NMDA receptors are stimulated [37], and turnover of gephyrin is regulated by calpain-1 activity [38]. Therefore, it is possible that gephyrin stability is also controlled by the activation of calpain-1 during NMDA stimulation [39]. However, it must be noted that the same NMDA stimulation (50 μM, with glycine and TTX) did not induce gephyrin declustering in cultured spinal cord neurons [40], in which calpain-1 is also activated by NMDA stimulation [41]. Thus, the molecular mechanism for this GABA_AR-independent gephyrin regulation remains to be elucidated by future studies.

Activity-dependent regulation of GABA_AR lateral diffusion and clustering at inhibitory synapses is mediated by Ca²⁺ influx and subsequent activation of calcineurin [11,12,13]. Our present findings provide several insights into the molecular mechanism of how Ca²⁺ signaling enhances GABA_AR lateral diffusion. In the present study, we found that GABA_AR diffusion and clustering were independent of gephyrin clustering during NMDA stimulation in the presence of CysA. This finding strongly suggests that calcineurin-dependent regulation of GABA_AR mobility does not require gephyrin. Because alterations in receptor-scaffold interactions can modulate the lateral diffusion of receptors [15], we propose the existence of other GABA_AR-interacting protein(s) that contribute to GABA_AR stabilization in a gephyrin-independent manner. GABA_AR accumulation at the inhibitory synapse occurs before gephyrin accumulation during synaptogenesis in spinal cord neurons [42], suggesting the existence of a gephyrin-independent stabilization mechanism of GABA_ARs. This gephyrin-independent pathway may enhance GABA_AR lateral diffusion via the calcineurin-dependent dephosphorylation of Ser327 in the GABA_AR γ2 subunit [12]. We speculate that the dephosphorylation of Ser327 upon neuronal excitation induces the dissociation of unidentified GABA_AR-associating protein(s) from GABA_ARs, which leads to the observed increase in GABA_AR lateral mobility.

The Ca²⁺-dependent increase in GABA_AR lateral mobility is involved in synaptic plasticity at inhibitory synapses that may underlie neuronal disorders resulting from pathological disinhibition [11,12]. Therefore, elucidating the detailed molecular mechanism of the gephyrin-independent regulation of GABA_AR lateral mobility might contribute not only to understanding the basis of learning and memory but also to discovering therapeutic targets for neuropathies such as epilepsy.

Materials and Methods

Ethics statement

All animal procedures in this study were performed in accordance with the guidelines issued by the Japanese Ministry of Education, Culture, Sports, Science and Technology. All animal procedures in this study were approved by the Animal Experiment Committee of the RIKEN (H23-2-204). All efforts

were made to minimize animal suffering and reduce the number of animals used.

Anti-GABA_AR γ2 subunit antibody production

The rabbit anti-GABA_AR γ2 subunit antibody (anti-GABA_ARγ2) was raised against the peptide “QKSDDDDYE-DYASNKTWVLTTPKVPEGDVTV(C)” corresponding to amino acid residues 39–67 of the rat GABA_AR γ2 subunit, as shown previously [43]. The peptide was synthesized by the Support Unit for Bio-material Analysis at the RIKEN BSI Research Resources Center (RRC) and was subsequently injected into rabbits to obtain the antibody by the Support Unit for Animal Resources Development at the RIKEN BSI RRC.

The specificity of the antibody was confirmed using HeLa cells (RIKEN BioResource Center, Ibaraki, Japan) expressing α1, β3, and γ2 subunits of GABA_AR (Fig. 1A and C). HeLa cells were plated onto 18-mm diameter glass coverslips and cultured in DMEM (Nacalai Tesque, Kyoto, Japan) supplemented with 10% fetal bovine serum and antibiotics. For transfection, a coverslip in 1 ml culture medium was incubated with the transfection mixture containing 100 μl OPTI-MEM (Invitrogen, Tokyo, Japan), mixture of DNA (α1, β3, γ2; 0.7 μg each), and 4.2 μl TransIT-LT1 (Mirus, WI, USA) for 24 h before observation. Plasmids encoding α1, β3, and γ2 subunits of GABA_AR were generated by subcloning the coding region into the mammalian expression vector [pcDNA3.1/Zeo(+/-); Invitrogen] using FANTOM3 clones as PCR templates (α1: C630037M06; β3: C630014N19; γ2: B930018F17 and C230063G02) [44].

Primary cultures

Primary cultures of hippocampal neurons co-cultured with astrocytes were prepared from E18–21 Wistar rat embryos as previously described [45] with some modifications. Hippocampal cells were dissociated in plating medium comprising minimum essential medium (MEM; Invitrogen) supplemented with B27 (Invitrogen), 2 mM L-glutamine, 1 mM sodium pyruvate (Invitrogen), and antibiotics, and were plated at a density of 1.4 × 10⁵ cells/ml onto 18-mm diameter glass coverslips precoated with 0.04% polyethyleneimine (Sigma, Tokyo, Japan). Three days after plating, the culture medium was replaced with maintenance medium comprising Neurobasal-A medium (Invitrogen) supplemented with B27, 2 mM L-glutamine, and antibiotics. Cells were cultured for 21–27 days *in vitro* before the experiments. At least three independent cultures were used for each experiment.

Drug treatment

To increase excitatory activity, cultured hippocampal neurons were incubated with 50 μM 4AP (Nacalai Tesque) or 50 μM NMDA (Tocris, MO, USA), glycine (5 μM), and TTX (1 μM; Tocris) at 37°C in the imaging medium comprising MEM without phenol red (Invitrogen), 20 mM HEPES, 33 mM glucose, 2 mM glutamine, 1 mM sodium pyruvate, and B27. For time-course analysis of cluster recovery, neurons were treated with 50 μM 4AP for 10 min and subsequently incubated with the imaging medium for 0–15 min before fixation. For QD-SPT experiments, 4AP (final concentration, 50 μM) was added to the imaging medium immediately before recording. For Ca²⁺ imaging, recording were done for 1 min in the absence of drugs, then drugs were bath applied to the cells during the recording.

Immunocytochemistry and quantitative analysis

For GABA_AR immunostaining of cultured neurons with drug treatment, endogenous GABA_ARs on cultured hippocampal

neurons were labeled with our $\gamma 2$ antibodies by incubating live cells with 2.0 $\mu\text{g/ml}$ antibody diluted in imaging medium for 30 min at 37°C. Subsequently, cells were stimulated by 4AP or NMDA and fixed with 4% (w/v) paraformaldehyde (PFA) in PBS-0.02% NaN_3 at room temperature (24–26°C) for 15 min. After permeabilization with 0.1% triton X-100 for 3 min and incubation with 5% (w/v) bovine serum albumin (BSA; Sigma) for 30 min to block nonspecific staining, cells were labeled with the mouse anti-synapsin I antibody (1:3000; Synaptic Systems, Goettingen, Germany) in 2.5% BSA for 60 min. After washes, the cells were incubated in Alexa Fluor®-conjugated secondary antibodies (5–10 $\mu\text{g/ml}$, Alexa Fluor 488 or Alexa Fluor 594; Invitrogen) for 30 min, washed, and mounted on slides with Vectashield (Vector Laboratories, CA, USA). In the experiments using the calcineurin inhibitor CysA (1 μM ; Santa Cruz Biotechnology, CA, USA), cells were incubated with our $\gamma 2$ antibodies (2.0 $\mu\text{g/ml}$) for 30 min in the presence of drug (i.e., 4AP, NMDA+TTX+Gly, CysA) and subsequently fixed by 4% PFA. After fixation, the procedures were the same as those of experiments without CysA treatment. In some experiments (Fig. S1E), GABA_AR was labeled with commercially available rabbit anti- $\gamma 2$ subunit antibodies (6.0 $\mu\text{g/ml}$; Alomone Labs, Jerusalem, Israel), which were used in a previous study [11]. GABA_ARs on the GABA_AR-expressing HeLa cells were labeled with our custom-made anti-GABA_AR $\gamma 2$ antibody (0.8 $\mu\text{g/ml}$) as described above, and nuclei of HeLa cells were stained with DAPI.

For labeling of gephyrin, cells were fixed with 4% PFA after drug stimulation and permeabilized with 0.1% Triton X-100. After blocking with 5% BSA, cells were incubated with anti-gephyrin antibody (0.33 $\mu\text{g/ml}$, clone mAb7a; Synaptic Systems) and the rabbit polyclonal anti-synapsin I antibody (1:400; Millipore, MA, USA) in the presence of 2.5% BSA for 90 min, and subsequently labeled with Alexa Fluor 488 or Alexa Fluor 594 (5–10 $\mu\text{g/ml}$; Invitrogen).

Immunofluorescence from isolated neurons was acquired on an inverted microscope (IX-70; Olympus, Tokyo, Japan) equipped with a Plan Apo 60 \times oil immersion objective with a numerical aperture (NA) of 1.42 (Olympus), cooled CCD camera (Orca-II-ER; Hamamatsu Photonics, Shizuoka, Japan), and appropriate filter sets for Alexa Fluor 488 (ex: 480 \pm 10 nm, em: 530 \pm 20 nm) and Alexa Fluor 594 (ex: 535 \pm 15 nm, em: 580 nm long pass). All images from a given culture were acquired with the same subsaturation exposure time.

Quantification of GABA_AR-, gephyrin-, and synapsin-associated immunofluorescence was performed using “Integrated Morphometry Analysis” function of the MetaMorph software (Molecular Device Japan, Tokyo, Japan). GABA_AR- and gephyrin-immunoreactive clusters and synapsin-positive presynapses were defined by processing images with multidimensional image analysis (MIA) interface, i.e., a 2D object segmentation by wavelet transform [46] and “auto threshold for light object (isodata method)” function of MetaMorph. Synaptic GABA_AR or gephyrin clusters were defined as clusters that overlapped at least 1 pixel with presynaptic terminals. For each culture, all cluster fluorescence intensity was normalized to the average value in control cells.

QD-SPT experiments

Neurons were incubated with the custom-made anti-GABA_AR $\gamma 2$ antibody (2.0 $\mu\text{g/ml}$) for 5 min, washed, and incubated with the biotinylated anti-rabbit Fab antibody (2.2 $\mu\text{g/ml}$; Jackson ImmunoResearch, PA, USA) for 5 min. Following washes, the coverslips were incubated with 1.0 nM streptavidin-coated QDs emitting at 605 nm or 625 nm (Invitrogen) in borate buffer for

1 min [29]. After washes, functional presynaptic boutons were labeled with 2 μM FM4-64 (Invitrogen) in imaging medium containing 40 mM KCl for 15 s. Incubation with antibodies and washes were performed at 37°C in the imaging medium.

The diffusive behavior of GABA_AR-QD and FM4-64 signals was recorded at 37°C in the imaging medium using an inverted microscope (IX-71, Olympus) equipped with an oil immersion objective (NA 1.45, 60 \times ; Olympus) and an EM-CCD camera (C9100; Hamamatsu Photonics) or an inverted microscope (IX-70; Olympus) equipped with an oil immersion objective (NA 1.42, 60 \times ; Olympus) and cooled CCD camera (Orca-II-ER; Hamamatsu Photonics). Fluorescent signals were detected using appropriate filter sets for QD (ex: 455 \pm 70 nm, em: 605 \pm 20 nm) and FM4-64 (ex: 535 \pm 15 nm, em: 580 nm long pass). GABA_AR-QD lateral diffusion was recorded with an integration time of 76 ms with 512 consecutive frames (38.9 s). All recordings were taken within 30 min.

Data analysis for QD-SPT experiments

The trajectory of GABA_AR-QD was obtained by cross-correlating images with a Gaussian model of the point spread function [47], and diffusion coefficients and confinements were calculated using TI workbench software written by Dr. T. Inoue (Waseda University), as described previously [11]. Only single QDs identified by intermittent fluorescence (i.e., blinking) were analyzed. The synaptic area was defined by processing FM4-64 images with wavelet decomposition [46]. GABA_AR-QDs were classified as “synaptic” when overlapping with synaptic area+2 pixels (284 nm). For the calculation of diffusion parameters in the synapse except for synaptic dwell time, the longest sub-trajectories of single GABA_AR-QDs with greater than or equal to 30 points in each compartment were taken into account.

To obtain the diffusion parameters, such as the diffusion coefficient and confinement size, values of the mean square displacement (MSD) plot versus time were calculated for each trajectory by applying the following equation:

$$MSD(n\tau) = \frac{1}{N-n} \sum_{i=1}^{N-n} \left[(x((i+n)\tau) - x(i\tau))^2 + (y((i+n)\tau) - y(i\tau))^2 \right] \quad (1)$$

([48]), where τ is the acquisition time, N is the total number of frames, and n and i are positive integers with n representing the time increment. Diffusion coefficients (D) were calculated by fitting first four points of the MSD versus time curves with the following equation:

$$MSD(n\tau) = 4Dn\tau + b, \quad (2)$$

where b is a constant reflecting the spot localization accuracy. In this system, GABA_AR-QDs with a diffusion coefficient (D) less than 0.0002 $\mu\text{m}^2/\text{s}$ were defined as immobile.

The confinement domain size, in which the diffusion of GABA_AR-QD was restricted, was obtained by fitting the MSD- $n\tau$ plot to the following equation:

$$MSD(n\tau) = \frac{L^2}{3} \left(1 - \exp\left(-\frac{12Dn\tau}{L^2}\right) \right) + 4D_{mac}n\tau \quad (3)$$

[30], where L^2 is the confined area in which diffusion is restricted, and D_{mac} is the diffusion coefficient on a long time scale. The

diffusion of GABA_AR-QD with MSD-nt plot that does not apply $|D-D_{\text{mac}}| < 0.1 \times D$ or $L < 0.001$ was defined as restricted motion, and only GABA_AR-QDs meeting this criteria were considered for calculations of confinement domain sizes [49].

The GABA_AR-QD dwell time inside the synapse was defined as the duration of synaptic sub-trajectories.

GABA_AR XL experiments

GABA_ARs on the cell surface were cross-linked by incubating neurons with the anti- $\gamma 2$ subunit antibody (8.0 $\mu\text{g}/\text{ml}$; Alomone Labs) for 10 min, washing, and incubating with Alexa Fluor[®]-conjugated anti-rabbit antibodies (20 $\mu\text{g}/\text{ml}$; Invitrogen) for 5 min in the imaging medium. Cells were further incubated with the biotinylated anti-rabbit Fab antibody and streptavidin-coated QDs for QD-SPT, or fixed and subsequently immunolabeled with the gephyrin antibody for quantitative immunocytochemistry, as mentioned previously. In all experiments, it was confirmed that surface GABA_ARs were successfully cross-linked by fluorescence from GABA_AR-associated clusters (Fig. 4A).

Ca²⁺ imaging

Neurons were loaded with 0.5 μM fluo-4 AM (Invitrogen) for 5 min at 37°C. Fluo-4 fluorescence was acquired at 0.2 Hz with a 200-ms exposure at room temperature (24–26°C), with an inverted microscope (IX-70; Olympus) equipped with a 40 \times objective (NA 0.85, UPlanApo; Olympus), a cooled CCD camera (Orca-II-ER; Hamamatsu Photonics), and appropriate filters (ex, 480 \pm 10 nm; em, 530 \pm 20 nm). For longer recording (Figs. 6E and 7E), images were further acquired at 0.1 Hz from 6 min to 15 min after drug application. Data were analyzed using a TI Workbench. The ratio of the fluorescence intensities F/F_0 , where F is a fluorescence intensity and F_0 is the intensity at $t=0$, was calculated after subtraction of the background fluorescence. To estimate the level of Ca²⁺ elevation, the area under the curve was calculated using Igor Pro software (WaveMetrics, OR, USA).

Statistical analysis and image preparation

Statistical differences of data in the time course were determined using the Kruskal–Wallis (for the diffusion coefficient)

References

- Moss SJ, Smart TG (2001) Constructing inhibitory synapses. *Nat Rev Neurosci* 2: 240–250.
- Kilman V, van Rossum MC, Turrigiano GG (2002) Activity deprivation reduces miniature IPSC amplitude by decreasing the number of postsynaptic GABA(A) receptors clustered at neocortical synapses. *J Neurosci* 22: 1328–1337.
- Nusser Z, Cull-Candy S, Farrant M (1997) Differences in synaptic GABA(A) receptor number underlie variation in GABA mini amplitude. *Neuron* 19: 697–709.
- Marsden KC, Beattie JB, Friedenthal J, Carroll RC (2007) NMDA receptor activation potentiates inhibitory transmission through GABA receptor-associated protein-dependent exocytosis of GABA(A) receptors. *J Neurosci* 27: 14326–14337.
- Marsden KC, Shemesh A, Bayer KU, Carroll RC (2010) Selective translocation of Ca²⁺/calmodulin protein kinase IIalpha (CaMKIIalpha) to inhibitory synapses. *Proc Natl Acad Sci U S A* 107: 20559–20564.
- Goodkin HP, Joshi S, Mtchedlishvili Z, Brar J, Kapur J (2008) Subunit-specific trafficking of GABA(A) receptors during status epilepticus. *J Neurosci* 28: 2527–2538.
- Lu YM, Mansuy IM, Kandel ER, Roder J (2000) Calcineurin-mediated LTD of GABAergic inhibition underlies the increased excitability of CA1 neurons associated with LTP. *Neuron* 26: 197–205.
- Naylor DE, Liu H, Wasterlain CG (2005) Trafficking of GABA(A) receptors, loss of inhibition, and a mechanism for pharmacoresistance in status epilepticus. *J Neurosci* 25: 7724–7733.
- Terunuma M, Xu J, Vitahlani M, Sieghart W, Kittler J, et al. (2008) Deficits in phosphorylation of GABA(A) receptors by intimately associated protein kinase C activity underlie compromised synaptic inhibition during status epilepticus. *J Neurosci* 28: 376–384.
- Wang J, Liu S, Haditsch U, Tu W, Cochrane K, et al. (2003) Interaction of calcineurin and type-A GABA receptor gamma 2 subunits produces long-term depression at CA1 inhibitory synapses. *J Neurosci* 23: 826–836.
- Bannai H, Lévi S, Schweizer C, Inoue T, Launey T, et al. (2009) Activity-dependent tuning of inhibitory neurotransmission based on GABA_AR diffusion dynamics. *Neuron* 62: 670–682.
- Muir J, Arancibia-Carcamo IL, MacAskill AF, Smith KR, Griffin LD, et al. (2010) NMDA receptors regulate GABA_A receptor lateral mobility and clustering at inhibitory synapses through serine 327 on the gamma2 subunit. *Proc Natl Acad Sci U S A* 107: 16679–16684.
- Luscher B, Fuchs T, Kilpatrick CL (2011) GABA_A receptor trafficking-mediated plasticity of inhibitory synapses. *Neuron* 70: 385–409.
- Bruneau EG, Esteban JA, Akaaboune M (2009) Receptor-associated proteins and synaptic plasticity. *FASEB J* 23: 679–688.
- Gerrow K, Triller A (2010) Synaptic stability and plasticity in a floating world. *Curr Opin Neurobiol* 20: 631–639.
- Mukherjee J, Kretschmannova K, Gouzer G, Maric HM, Ramsden S, et al. (2011) The Residence Time of GABA_ARs at Inhibitory Synapses Is Determined by Direct Binding of the Receptor $\alpha 1$ Subunit to Gephyrin. *J Neurosci* 31: 14677–14687.
- Tretter V, Jacob TC, Mukherjee J, Fritschy JM, Pangalos MN, et al. (2008) The clustering of GABA(A) receptor subtypes at inhibitory synapses is facilitated via the direct binding of receptor alpha 2 subunits to gephyrin. *J Neurosci* 28: 1356–1365.
- Tretter V, Kerschner B, Milenkovic I, Ramsden SL, Ramerstorfer J, et al. (2011) Molecular basis of the GABA_A receptor $\alpha 3$ subunit interaction with gephyrin. *J Biol Chem*.
- Fritschy JM, Harvey RJ, Schwarz G (2008) Gephyrin: where do we stand, where do we go? *Trends Neurosci* 31: 257–264.

and one-way ANOVA ($p=0.05$) tests, followed by Tukey's post-hoc tests (for others). For comparisons between two groups, the Mann–Whitney U test or Welch's t -test were performed as indicated. All statistical analysis was performed using Kaleida-Graph (Synergy Software, PA, USA). Images were prepared for printing using MetaMorph, Adobe Photoshop, and Adobe Illustrator.

Supporting Information

Figure S1 Specificity of the anti-GABAAR $\gamma 2$ subunit antibody.

(PDF)

Figure S2 Recovery of GABAAR and gephyrin immunofluorescence after 4AP washout.

(PDF)

Figure S3 Lateral diffusion of GABAAR with or without FM4–64 labeling.

(PDF)

Acknowledgments

We thank the members of the Research Resource Center for invaluable technical support in the development of the GABA_AR $\gamma 2$ antibody and for providing FANTOM clones. We specially thank Takafumi Inoue, Maxim Dahan, Victor Racine, and Jean-Baptiste Sibarita for data analysis programs, and Charles Yokoyama, Chihiro Hisatsune, Yoshiyuki Yamada, and Masahiro Enomoto for their valuable comments on the manuscript. We thank two anonymous reviewers for their insightful and constructive comments on the manuscript.

Author Contributions

Conceived and designed the experiments: HB AT KM. Performed the experiments: FN HB MA. Analyzed the data: FN HB. Contributed reagents/materials/analysis tools: FN HB KF. Wrote the paper: FN HB MA AT KM.

20. Jacob TC, Bogdanov YD, Magnus C, Saliba RS, Kittler JT, et al. (2005) Gephyrin regulates the cell surface dynamics of synaptic GABA_A receptors. *J Neurosci* 25: 10469–10478.
21. Kneussel M, Brandstatter JH, Laube B, Stahl S, Muller U, et al. (1999) Loss of postsynaptic GABA(A) receptor clustering in gephyrin-deficient mice. *J Neurosci* 19: 9289–9297.
22. Essrich C, Lorez M, Benson JA, Fritschy JM, Luscher B (1998) Postsynaptic clustering of major GABA_A receptor subtypes requires the gamma 2 subunit and gephyrin. *Nat Neurosci* 1: 563–571.
23. Kralic JE, Sidler C, Parpan F, Homanics GE, Morrow AL, et al. (2006) Compensatory alteration of inhibitory synaptic circuits in cerebellum and thalamus of gamma-aminobutyric acid type A receptor alpha 1 subunit knockout mice. *J Comp Neurol* 495: 408–421.
24. Li RW, Yu W, Christie S, Miralles CP, Bai J, et al. (2005) Disruption of postsynaptic GABA receptor clusters leads to decreased GABAergic innervation of pyramidal neurons. *J Neurochem* 95: 756–770.
25. Panzanelli P, Gunn BG, Schlatter MC, Benke D, Tyagarajan SK, et al. (2011) Distinct mechanisms regulate GABA_A receptor and gephyrin clustering at perisomatic and axo-axonic synapses on CA1 pyramidal cells. *J Physiol*.
26. Schweizer C, Balsiger S, Bluethmann H, Mansuy IM, Fritschy JM, et al. (2003) The gamma 2 subunit of GABA(A) receptors is required for maintenance of receptors at mature synapses. *Mol Cell Neurosci* 24: 442–450.
27. Studer R, von Boehmer L, Haenggi T, Schweizer C, Benke D, et al. (2006) Alteration of GABAergic synapses and gephyrin clusters in the thalamic reticular nucleus of GABA_A receptor alpha3 subunit-null mice. *Eur J Neurosci* 24: 1307–1315.
28. Stelzer A, Slater NT, ten Bruggencate G (1987) Activation of NMDA receptors blocks GABAergic inhibition in an in vitro model of epilepsy. *Nature* 326: 698–701.
29. Bannai H, Lévi S, Schweizer C, Dahan M, Triller A (2006) Imaging the lateral diffusion of membrane molecules with quantum dots. *Nat Protoc* 1: 2628–2634.
30. Kusumi A, Sako Y, Yamamoto M (1993) Confined lateral diffusion of membrane receptors as studied by single particle tracking (nanovid microscopy). Effects of calcium-induced differentiation in cultured epithelial cells. *Biophys J* 65: 2021–2040.
31. Heine M, Groc L, Frischknecht R, Beique JC, Lounis B, et al. (2008) Surface mobility of postsynaptic AMPARs tunes synaptic transmission. *Science* 320: 201–205.
32. Renner M, Lacor PN, Velasco PT, Xu J, Contractor A, et al. (2010) Deleterious effects of amyloid beta oligomers acting as an extracellular scaffold for mGluR5. *Neuron* 66: 739–754.
33. Lévi S, Logan SM, Tovar KR, Craig AM (2004) Gephyrin is critical for glycine receptor clustering but not for the formation of functional GABAergic synapses in hippocampal neurons. *J Neurosci* 24: 207–217.
34. Dobie FA, Craig AM (2011) Inhibitory synapse dynamics: coordinated presynaptic and postsynaptic mobility and the major contribution of recycled vesicles to new synapse formation. *J Neurosci* 31: 10481–10493.
35. Lévi S, Grady RM, Henry MD, Campbell KP, Sanes JR, et al. (2002) Dystroglycan is selectively associated with inhibitory GABAergic synapses but is dispensable for their differentiation. *J Neurosci* 22: 4274–4285.
36. Sekimoto K, Triller A (2009) Compatibility between itinerant synaptic receptors and stable postsynaptic structure. *Phys Rev E Stat Nonlin Soft Matter Phys* 79: 031905.
37. Kawasaki BT, Hoffman KB, Yamamoto RS, Bahr BA (1997) Variants of the receptor/channel clustering molecule gephyrin in brain: distinct distribution patterns, developmental profiles, and proteolytic cleavage by calpain. *J Neurosci Res* 49: 381–388.
38. Tyagarajan SK, Ghosh H, Yevens GE, Nikonenko I, Ebeling C, et al. (2011) Regulation of GABAergic synapse formation and plasticity by GSK3beta-dependent phosphorylation of gephyrin. *Proc Natl Acad Sci U S A* 108: 379–384.
39. Tyagarajan SK, Fritschy JM (2010) GABA(A) receptors, gephyrin and homeostatic synaptic plasticity. *J Physiol* 588: 101–106.
40. Lévi S, Schweizer C, Bannai H, Pascual O, Charrier C, et al. (2008) Homeostatic regulation of synaptic GlyR numbers driven by lateral diffusion. *Neuron* 59: 261–273.
41. Das A, Sribnick EA, Wingrave JM, Del Re AM, Woodward JJ, et al. (2005) Calpain activation in apoptosis of ventral spinal cord 4.1 (VSC4.1) motoneurons exposed to glutamate: calpain inhibition provides functional neuroprotection. *J Neurosci Res* 81: 551–562.
42. Dumoulin A, Lévi S, Riveau B, Gasnier B, Triller A (2000) Formation of mixed glycine and GABAergic synapses in cultured spinal cord neurons. *Eur J Neurosci* 12: 3883–3892.
43. Benke D, Mertens S, Trzeciak A, Gillissen D, Mohler H (1991) GABA_A receptors display association of gamma 2-subunit with alpha 1- and beta 2/3-subunits. *J Biol Chem* 266: 4478–4483.
44. Carninci P, Kasukawa T, Katayama S, Gough J, Frith MC, et al. (2005) The transcriptional landscape of the mammalian genome. *Science* 309: 1559–1563.
45. Goslin K, Asmussen H, Banker G (1998) In Culturing nerve cells; Banker G, Goslin K, eds. MIT press, Cambridge.
46. Racine V, Sachse M, Salamero J, Fraiser V, Trubuil A, et al. (2007) Visualization and quantification of vesicle trafficking on a three-dimensional cytoskeleton network in living cells. *J Microsc* 225: 214–228.
47. Bonneau S, Cohen L, Dahan M (2004) A multiple target approach for single quantum dot tracking. *Proceedings of the IEEE International Symposium on Biological Imaging*. 664 p.
48. Saxton MJ, Jacobson K (1997) Single-particle tracking: applications to membrane dynamics. *Annu Rev Biophys Biomol Struct* 26: 373–399.
49. Ehrensperger MV, Hanus C, Vannier C, Triller A, Dahan M (2007) Multiple association states between glycine receptors and gephyrin identified by SPT analysis. *Biophys J* 92: 3706–3718.